Kinetics of Reduction of Ferrous Oxide with Hydrogen in a Fluidized Bed at Steady State

JEROME FEINMAN and THOMAS D. DREXLER

U.S. Steel Corporation, Monroeville, Pennsylvania

The kinetics of the reduction of ferrous oxide with hydrogen in a steady state fluidized bed *have been correlated with a rate equation based on a reaction controlled at the oxide-metal* interface and on a differential material balance which assumes that a close approach to piston flow prevails. The correlation gives an enthalpy of activation of 29,500 b.t.u./lb. mole for the reaction, which is in good agreement with McKewan's reported value of 27,500 b.t.u./lb. mole. The relationships developed are used to predict the effect of the important independent variables on the over-all kinetics of the system.

Equilibrium relationships for the system iron:oxygen:hydrogen are well established (*1, 2, 3*) and can be used to define equilibrium compositions for any combination without regard to the physical structure of the iron ore. The kinetics of iron-ore reduction with hydrogen however are not so easy to define. Although recent studies by McKewan (*4, 5*) have shown that the reduction of iron oxide by hydrogen is controlled at the oxide-metal interface, the rate-controlling step has not yet been established for any of the possible mechanisms. In addition any generalized kinetic mechanism for this heterogeneous system is confounded by the physical differences among the many ores processed. A rate equation, based on McKewan's hypothesis, was derived that fits most reported data. In the present paper this rate equation has been used to correlate the data from an experimental study of the continuous reduction of FeO with hydrogen in a fluidized bed.

THEORY

Most of the reported data on the kinetics of iron-ore reduction by hydrogen are based on experiments involving particles of known geometry in an isothermal environment where increases in gas flow did not significantly affect the rate of reduction. Following McKewan, consider a sphere of iron oxide of initial radius r_o and initial density d_o. Assume that the rate of formation of a uniform reaction-product layer is proportional to the receding surface area A of the remaining oxide. If W is the weight of the original material that has reacted, then

$$\frac{dW}{d\theta} = kA \qquad (1)$$

The constant k is a function of temperature, pressure, and gas composition and actually represents the rate at which a unit area of reacting surface loses oxygen. From this it follows that

$$r_o d_o f = k\theta \qquad (2)$$

where

$$f = \frac{r_o - r}{r_o}$$

The fractional reduction is defined as the oxygen removed, divided by the oxygen originally present as iron oxide. R_f is related to f as follows:

$$f = 1 - (1 - R_f)^{1/3} \qquad (3)$$

When one defines S as the mole ratio of oxygen to iron in the particle, S is related to R_f by the following equation (when one considers $R_f = 0$ for ferrous oxide):

$$S = (1 - R_f) \qquad (4)$$

Substituting (3) and (4) for f in Equation (2) one gets

$$r_o d_o [1 - S^{1/3}] = k\theta \qquad (5)$$

The same equation would apply to a cube the side of which equalled $2r_o$. The reduction rate for any particle similar in shape to a sphere or a cube can be approximated by Equation (5).

In accordance with the theory of absolute reaction rates (*6*) the rate of a reaction taking place on a unit area of surface can be expressed by the following equation:

$$k = K_o (\pi_i C_i) k' \qquad (6)$$

The specific rate constant k' is defined as

$$k' = \kappa \frac{k_B T}{h} \exp - \frac{\Delta H^\ddagger}{RT} \exp \frac{\Delta S^\ddagger}{R} \qquad (7)$$

For the case of reduction of iron oxide in pure hydrogen the rate is directly proportional to the hydrogen pressure for pressures less than 2 atm.; therefore

$$(\pi_i C_i) \sim P_{H_2} \qquad (8)$$

Substituting (7) for k' and (8) for $(\pi_i C_i)$ in (6) one obtains

$$k = Q P_{H_2} \qquad (9)$$

where

$$Q = K_o \kappa \frac{k_B T}{h} \exp - \frac{\Delta H^\ddagger}{RT} \exp \frac{\Delta S^\ddagger}{R}$$

If one assumes that the rate constant k decreases essentially linearly with increasing water-vapor concentration and becomes zero at the equilibrium concentration,[*] k can be expressed as a function of the partial pressure of water vapor and hydrogen by

$$k = Q \left(P_{H_2} - \frac{1}{K} P_{H_2O} \right)$$

This can be converted to

$$k = Q\pi \left[1 - y_n - \left(\frac{K+1}{K} \right) y \right] \qquad (10)$$

The rate constant k is defined generally for any gas composition. Taking the derivative of (5) with respect to θ one gets

$$k = \frac{-r_o d_o}{3} S^{-2/3} \frac{dS}{d\theta} \qquad (11)$$

When one equates (10) and (11), $dS/d\theta$, the rate at which a given particle loses oxygen, can be expressed as

$$\frac{dS}{d\theta} = - \frac{3}{r_o d_o} Q\pi S^{2/3} \left[1 - y_n - \left(\frac{K+1}{K} \right) y \right] \qquad (12)$$

Equation (12) defines the kinetics of reduction of a single sphere in general (that is, for any combination of variables where reduction is controlled at an oxide-metal surface). It is reasonable to assume that it can be used to describe the over-all kinetics in a fluidized bed where many different particles and environments are encountered. The problem is simplified when the physical characteristics of a continuous fluidized system at steady state are considered. Solid samples taken from the top and bottom of a steady state fluidized bed in which iron oxide is being reduced with hydrogen have the same chemical composition. The solids in the bed may therefore

---

[*] McKewan has found that this is not true for temperatures below the triple point on the equilibrium diagram (1050°F) (*7*); however, he has found that it is true for the temperatures used in these experiments (*8*).

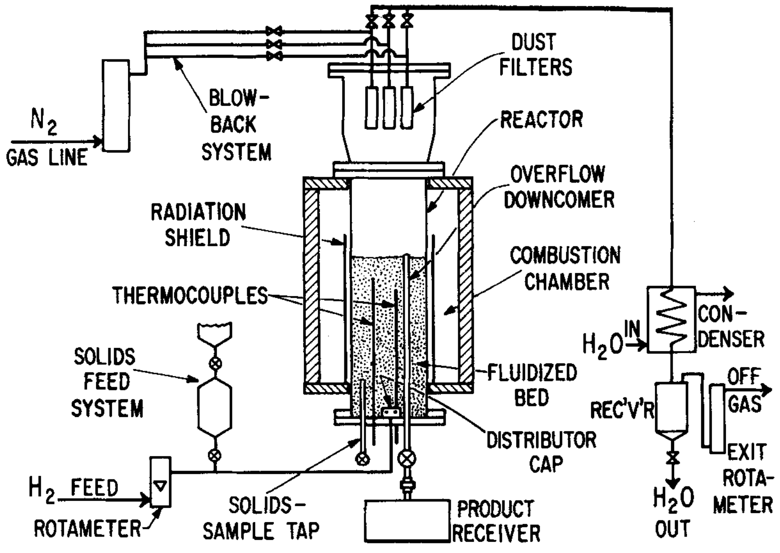

Fig. 1. Diagram of experimental apparatus.

be assumed to behave as if they are perfectly mixed, so that S is invariant with time and position. The gas flow cannot be represented so clearly. Much research has been done since the original tracer studies by Gilliland and Mason (9), and many models to describe the flow of gas through fluidized beds have been proposed as the result of these investigations. For example Danckwerts (*10*) concluded that the distribution of residence times for the gas flowing through a commercial fluidized-catalyst regenerator is much closer to piston flow than to complete mixing. Handlos et al. (*11*) on the other hand are convinced that the distribution of residence times for the gas in a similar regenerator follows the complete mixing distribution more closely. Finally there are a number of investigators who characterize the gas flow by models between these extremes.

It is believed that the distribution of residence times for the gas flow in this system is represented closely by assuming piston flow. This assumption is based on the following observations:

1. The approach to equilibrium for the exit gas in all runs was between 0.65 and 0.90 (approach to equilibrium is directly proportional to residence time and bed temperature; thus the lower values occur with lower-temperature operation, shallow beds, and higher gas rates). Because the reduction of iron oxide by hydrogen between 1,100° and 1,300°F. is a slow process (in comparison with burning carbon off a catalyst surface), these relatively high approaches to equilibrium are not consistent with complete mixing of the gases.

2. Visual observations of a fluidized bed of reduced iron-oxide particles during cold studies in a 6-in. diameter glass column show that there is vigorous slugging, with bubbles as tall as 10 in. appearing continuously at all levels. The bubbles, which are bounded by the column wall, move upward as solids rain down through the roof of the bubble. This type of fluidization, which is characteristic of iron oxide and reduced iron oxide, does not permit very much back mixing of gases as appears to happen with the more particulate fluidization found with cracking catalysts.

The heat transfer characteristics of fluidized beds also justify the assumption that the bed is isothermal (*12, 13*). This assumption will be discussed in the next section.

TABLE 1. TYPICAL SIZE DISTRIBUTION OF SOLIDS

	Cumulative %					
Solid	20M	40M	60M	80M	100M	120M
FeO feed	3.8	15.9	29.2	42.1	51.4	65.0
Reduced product	2.1	11.7	23.4	37.8	48.5	66.1

The oxygen balance across a differential section of a continuous fluidized bed at steady state is, for unit area

$$\text{Input} - \text{Output} = \text{Accumulation.}$$

$$\text{Input} = Gy$$

$$\text{Output} = G\left(y + \frac{dy}{dV}dV\right) + \left\{\frac{-3}{r_o d_o}\,Q\overline{\pi}\,S^{2/3}\left[1 - y_n - \left(\frac{K+1}{K}\right)y\right]\right\}dV$$

$$\text{Accumulation} = o$$

Therefore

$$G\,\frac{dy}{dV} = \frac{3}{r_o d_o}\,Q\overline{\pi}\,S^{2/3}\left[1 - y_n - \left(\frac{K+1}{K}\right)y\right]$$

with boundary conditions

$$\begin{cases} V = 0, & y = y_B \\ V = V, & y = y_T \\ y_n = 0 \end{cases}$$

When $y_B = 0$ ($y_B = 0$ for these experiments)

$$\left(\frac{K}{K+1}\right)\ln\frac{1}{1-\left(\frac{K+1}{K}\right)y_T} = \frac{3\,Q\overline{\pi}\,S^{2/3}}{r_o d_o}\,\frac{V}{G} \tag{13}$$

The over-all material balance is

$$F\,(S_o - S) = Gy_T \tag{14}$$

Equations (13) and (14) enable evaluation of $Q/r_o d_o$.

So far it has been assumed that the bed consists of dense spheres having radius r_o. Actually the ore used in these experiments was a mixture of particles

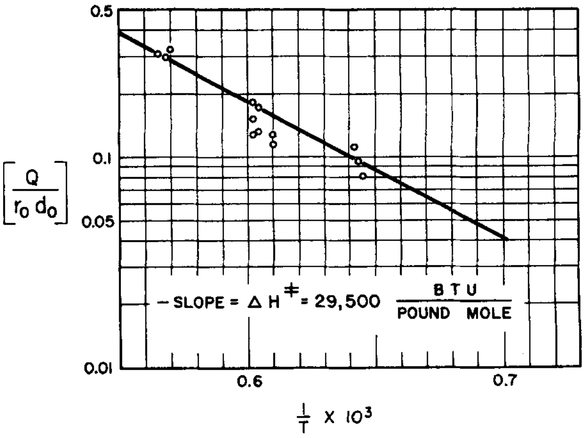

Fig. 2. Effect of temperature on rate function.

Table 2. Typical Operating Conditions and Steady State Results

Run	Bed temp., °F.	$\bar{\pi}$, atm.	Standpipe height, ft.	V, lb. moles Fe / sq. ft.	G, lb. moles / hr. sq. ft.	F, lb. moles Fe / hr. sq. ft.	S_o, atoms O/mole Fe	y_T, moles H_2O/tot moles	S, atoms O/mole Fe	K, $\frac{H_2O}{H_2}$ at Eq	Q/r_od_o	$1/T \times 10^3$, R^{-1}
548	1,095	1.37	4	5.02	4.65	1.09	1.043	0.145	0.372	0.326	0.0948	0.643
526	1,195	1.46	8	9.29	3.82	1.08	1.095	0.247	0.212	0.373	0.173	0.604
546	1,310	1.47	6	7.24	4.59	1.32	1.043	0.258	0.146	0.427	0.309	0.565

of many sizes and shapes, all very porous. The group $[Q/r_od_o]$ is therefore thought of as representing the average kinetic and geometric properties of the ore. For example r_o would represent an average radius for all the grains making up the particles, and d_o would represent the average original density of these grains. This representation for $[Q/r_od_o]$ is justified because laboratory experiments have shown that the reduction rate of the porous particles used in these studies is independent of particle size. This result is understandable because the individual grains making up the particles are much smaller than the particles themselves, and accessibility of these grains to the reactant gas is independent of their location in the particle.

A plot of $\ln[Q/r_od_o]$ vs. $1/T$ should give a straight line having slope equal to $-\Delta H^{\ddagger}$.

MATERIALS AND EXPERIMENTAL WORK

The apparatus used for the experimental work is shown schematically in Figure 1. The fluidized-bed reactor consisted of a 6-in. diameter stainless-steel cylinder 10 ft. high. A 2-ft. top section 12 in. in diameter, which was mounted directly on top of the reactor, contained the dust-collecting filters. The lower 9 ft. of the 6-in. diameter section was surrounded by a furnace chamber. The bottom flange was fitted with a gas-and-solid inlet as well as a solid sample tap.

The bed temperature was measured by chromel-alumel thermocouples in the bed and was automatically controlled by varying the amount of natural gas burned in the furnace combustion chamber.

Solid feed was introduced into the metered fluidizing gas through an adjustable slide valve, and the resulting solid-gas mixture entered the fluidized bed through a distribution cap on the bottom flange.

Dust entrained in the off gas was removed by porous stainless-steel filters mounted in the expanded section at the top of the bed. These filters were cleaned by blowing back with gas when the build-up of dust on the filter surface caused an excessive pressure drop.

The off gas leaving the filters passed through a water-cooled condenser where the water vapor was condensed and collected in a receiver and the remaining gas was discharged through the exit rotameter. The rate at which water collected was a measure of the rate of reduction achieved in the test.

The ferrous oxide used in these experiments was made from Venezuelan ore fines having about 3.0% gangue. Average cumulative size analyses for the ferrous oxide feed and the reduced product are shown in Table 1.

In a continuous fluidized-bed hydrogen reduction process the hydrogen can be utilized most effectively when reduction takes place in two steps (usually two separate beds with countercurrent flow between them) according to the following over-all reactions:

Step 1. $Fe_2O_3 + H_2 \rightleftarrows FeO + H_2O$

Step 2. $FeO + H_2 \rightleftarrows Fe + H_2O$

This two-step process takes advantage of the fact that off gas from Step 2 has more than enough capacity to complete the reaction in Step 1. In addition preliminary studies showed that the reduction of ferric oxide to ferrous oxide in Step 1 is relatively rapid, so that substantially ferrous oxide is produced over a wide range of temperatures and residence times of the reactants. The productive capacity of the process, particularly when operating temperatures are greater than 1,100°F., is therefore limited by the amount of oxygen that can be removed in Step 2. For these reasons the experimental emphasis was placed on the Step 2 system.

The final reduction step was simulated by continuously feeding ferrous oxide (prepared in previous studies) into a bed of highly reduced iron fluidized with pure hydrogen. Running these tests involved the following procedures.

A known weight of iron particles was introduced into the reactor, which was then fluidized at the desired gas rate, and the bed was heated to the operating temperature. The weight of solids in the bed was obtained by putting an excess amount in the initial charge and then weighing the excess, which was collected in the product receiver as the bed was raised to the operating temperature. Continuous feed of ferrous oxide was then started.

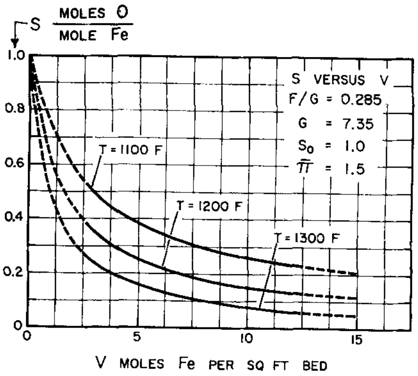

Fig. 3. Effect of bed inventory on product quality.

The run continued until sufficient steady state data were collected for calculating the material balance (usually about 8 hr.). At the end of the run the bed was cooled and weighed to obtain a check value for the weight of solids in the bed.

Because both reacting phases entered the bottom of the reactor at ambient temperatures, there was a low-temperature volume at the bottom of the bed. The assumption of isothermal conditions therefore needs justification. Thermocouples located at different axial positions in the bed showed this low-temperature zone to be at most about 1 ft. deep. This corresponds to between 12 and 25% of the total bed volume (standpipe heights were between 4 and 8 ft.). Sensible heat to heat the reactants to the reaction temperature and endothermic heat of reaction were added through the reactor walls. Therefore there was a high-temperature volume at the inner wall of the reactor. A high-temperature annulus having a thickness between 0.35 and 0.8 in. would result in a high-temperature volume range equal to the low-temperature volume range. The system thus tends to be self-compensating, and the assumption of isothermal conditions (the control thermocouple was always located in the isothermal zone of the reactor) should not be in serious error.

RESULTS AND DISCUSSION

Table 2 shows complete data for a run at each temperature level studied.* The vigorous slugging of the fluidized bed resulted in a bed inventory V that fluctuated somewhat. Although the solid feed rate F was fairly uniform, product weights collected during equal time intervals were variable; a high-weight period usually was followed by a low-weight period and vice versa. It is estimated however that V is accurate to ± 5%. The flow rate G was steady, and the rotameters used were accurate to ± 1% of their full-scale range, corresponding to a maximum

---

* Complete data for all the runs have been deposited as Document 6889 with the American Documentation Institute, Photoduplication Service, Library of Congress, Washington 25, D.C., and may be obtained for $1.25 for photoprints or for 35-mm. microfilm.

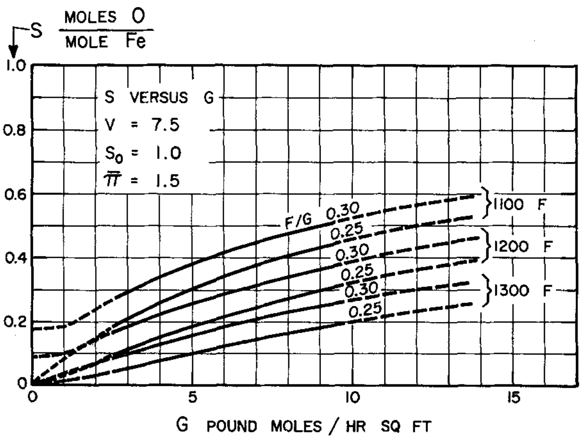

Fig. 4. Effect of gas rate on product quality.

error of ± 4% (for the low flow-rate runs). The values for S_o and S were calculated from chemical analyses. The analysis for total gangue content of the original ore had a maximum error of ± 0.2% gangue (for example, 3.0 ± 0.2%). Because total-iron determinations were all accurate to ± 0.1% iron, the maximum error for S_o was ±1.2% and for S about ± 5%. The outlet water-vapor concentration y_T was calculated from the total water collected during a given time interval plus the water vapor contained in the gas leaving the water receiver (this gas was assumed to be saturated at its exit temperature). The maximum error for y_T was less than ± 5%. Runs for which the over-all material balance did not check within 10% were not included. Usually these runs were associated with an operating period that was not long enough for attainment of steady state.

The rate functions $[Q/r_o d_o]$ are in fairly good agreement for the three temperature levels included in the experimental program. A plot of $\ln[Q/r_o d_o]$ vs. $1/T$ is shown in Figure 2. The relationship is very nearly linear, and the slope of the line drawn gives an enthalpy of activation of 29,500 B.t.u./lb. mole for the reaction. This is in good agreement with McKewan's reported value of 27,500 B.t.u./lb. mole.

Values of $[Q/r_o d_o]$ from Figure 2 and Equations (13) and (14) can be used to predict the effect of the important independent variables on the over-all kinetics of the system. For example the effect of bed inventory on product quality with constant gas rate and feed rate is shown in Figure 3. It can be seen that product quality increases with increasing bed inventory. The effect of gas rate on product quality with constant bed inventory and ratio of feed to gas is shown in Figure 4. This figure shows that product quality decreases with increasing throughput.

To sum up, data on the reduction of ferrous oxide with hydrogen in a steady state fluidized bed have been correlated with a rate equation based on a reaction controlled at the oxide-metal interface and on a differential material balance which assumes that a close approach to piston flow of the gas prevails. The kinetics of other steady state fluidized systems can be analyzed in this manner provided a rate equation is known and a close approach to piston flow prevails.

ACKNOWLEDGMENT

The authors express their thanks to W. M. McKewan of the Edgar C. Bain Laboratory for Fundamental Research for helpful discussions.

NOTATION

A = surface area of reaction interface
d_o = original density of oxide particle (or grain)
F = solid feed rate, lb. moles Fe/hr. sq.ft.
f = ratio of the thickness of the reduced iron layer to the initial radius of the particle (or grain)
G = gas rate, lb. moles/hr. sq.ft.
h = Planck's constant
K = equilibrium constant = $\left(\frac{p_{H_2O}}{p_{H_2}}\right)_{eq}$
K_o = proportionality constant from absolute reaction rate theory
k = general rate constant
k' = specific rate constant from absolute reaction rate theory
k_B = Boltzmann's constant
P = partial pressure, atm.
Q = $K_o \kappa \frac{k_B T}{h} \exp - \frac{\Delta H\ddagger}{RT} \exp \frac{\Delta S\ddagger}{R}$
R = gas law constant
R_f = fractional reduction, weight of oxygen removed divided by weight of oxygen originally present (R_f = 0 for iron oxide)
r = radius of reaction interface
r_o = initial radius of a particle (or grain)
S = mole ratio of oxygen to iron (O/Fe) in the particle
S_o = mole ratio O/Fe in feed
T = absolute temperature, °R.
V = bed inventory, lb. moles Fe/sq.ft.
W = weight of material that has reacted
y = mole fraction of component in gas

Greek Letters

θ = time, hr.
$(\pi_i C_i)$ = product of the concentrations of the reacting species
$\Delta H^\ddagger$ = enthalpy of activation
$\Delta S^\ddagger$ = entropy of activation
π = total pressure, atm.
$\bar{\pi}$ = average total pressure, atm.
κ = transmission coefficient from absolute reaction rate theory

Subscripts

B = bottom of bed
T = top of bed
n = inerts

LITERATURE CITED

1. Eastman, E. D., *J. Am. Chem. Soc.*, **44**, 975 (1922).
2. Emmett, P. H., and J. F. Schultz, *ibid.*, **52**, 4268 (1930).
3. *Ibid.*, **54**, 3780 (1932).
4. McKewan, W. M., *Trans. Am. Inst. Mining Met. Engrs.*, **212**, 791 (1958).
5. *Ibid.*, **218**, 2 (1960).
6. Glasstone, S., K. L. Laidler, H. Eyring, "Theory of Rate Processes," McGraw Hill, New York (1941).
7. McKewan, W. M., *Trans. Am. Inst. Mining Met. Engrs.*, **221**, 140 (1961).
8. ———, Paper presented at annual meeting of Metallurgical Society of Am. Inst. Mining Met. Engrs., St. Louis, Missouri (Feb., 1961).
9. Gilliland, E. R., and E. A. Mason, *Ind. Eng. Chem.*, **44**, 218 (1952).
10. Danckwerts, P. V., J. W. Jenkins, and G. Place, *Chem. Eng. Sci.*, **3**, 26 (1954).
11. Handlos, A. E., R. W. Kunstman, and D. O. Schissler, *Ind. Eng. Chem.*, **49**, 25 (1957).
12. Mickley, H. S., and C. A. Trilling, *ibid.*, **41**, 1135 (1949).
13. Leva, Max, Murray Weintraub, and Milton Grummer, *Chem. Eng. Progr.*, **45**, 563 (1949).

Manuscript received October 10, 1960; revision received April 7, 1961; paper accepted April 10, 1961. Paper presented at A.I.Ch.E. Tulsa meeting.